

EDGE ARTICLE

1

Cite this: DOI: 10.1039/c9sc06582b

5

All publication charges for this article have been paid for by the Royal Society of Chemistry

10

Received 31st December 2019
Accepted 28th February 2020

DOI: 10.1039/c9sc06582b
rsc.li/chemical-science

15

Introduction

“Smart” polymers that degrade in response to external triggers have found applications in many fields, including drug delivery, transient electronics, encapsulation and sensing.^{1–6} More recently, chain-shattering degradable polymers and self-immolative degradable polymers attracted considerable attention because their backbones can be completely degraded into small fragments with high sensitivity to different types of triggers including pH, light, and redox agents.^{7–16} However, both types of polymers require a stoichiometric amount of triggering agent and degradation rates are constant at best. Some self-immolative polymers suffer from slow or incomplete breakdown as side reactions can occur as the degradation proceeds down the polymer backbone. An alternative approach uses autocatalysis degradation chemistry wherein a specific catalytic trigger generates additional triggers for acceleration of degradation.^{17–21}

Phillips and coworkers reported that ROMP polymers with appropriate pendant chains could exhibit dramatic changes in macroscopic properties through amplified, self-propagating side-chain reactions.^{22,23} In particular, a global switch in hydro-phobicity and a change in the optical properties of a film occurred with local stimulation. In an effort to develop

Base-triggered self-amplifying degradable polyurethanes with the ability to translate local stimulation to continuous long-range degradation†

Yanhua Xu,^a Samya Sen,  Qiong Wu,  Xujia Zhong,^a Randy H. Ewoldt  and Steven C. Zimmerman  ^{*a}

A new type of base-triggered self-amplifying degradable polyurethane is reported that degrades under mild conditions, with the release of increasing amounts of amine product leading to self-amplified degradation. The polymer incorporates a base-sensitive Fmoc-derivative into every repeating unit to enable highly sensitive amine amplified degradation. A sigmoidal degradation curve for the linear polymer was observed consistent with a self-amplifying degradation mechanism. An analogous cross-linked polyurethane gel was prepared and also found to undergo amplified breakdown. In this case, a trace amount of localized base initiates the degradation, which in turn propagates through the material in an amplified manner. The results demonstrate the potential utility of these new generation polyurethanes in enhanced disposability and as stimuli responsive materials.

polymeric materials that might degrade with accelerated rate profiles and inspired by acid amplifier small molecules, we recently reported poly(3-iodopropyl)acetals that breakdown liberating HI.²⁴ In essence such polymers carry the seeds of their own destruction,²⁵ with liberated acid catalyzing further cleavage in an autocatalytic loop. It is important to determine the generality of the autocatalytic polymer degradation strategy by developing breakdown pathways using other triggers such as base, light and redox agents. Herein we report a new polyurethane that undergoes self-amplified degradation mediated by base and further show that in analogous gels, a small localized addition of base leads to rapid long-range breakdown (Fig. 1).

Results and discussion

As recently noted, base-degradable polymers are underdeveloped relative to acid-degradable polymers.^{26,27} In designing auto-catalytic base-degradable polyurethanes, the base amplifiers reported by Ichimura and others were considered.^{28–32} Within this class of small molecules, the Fmoc protected carbamate offered a convenient aromatic scaffold for functionalization and the potential for conventional polyurethane synthesis. The actual polyurethanes studied, **1** and **1c**, were prepared in six steps as shown in Scheme 1. Functionalization of the Fmoc aromatic ring was achieved through a Friedel-Crafts acylation after protection of alcohol with acetic anhydride, thus affording **4** or **5**. Acidic deprotection and reduction with $\text{BH}_3 \cdot \text{THF}$ produced intermediate **6** and **7**, which were further converted to diol monomer **8** and **9**, respectively, by selectively reducing the benzylic alcohol functional group with

^aDepartment of Chemistry, University of Illinois at Urbana-Champaign, Urbana, Illinois 61801, USA. E-mail: sczimmer@illinois.edu

^bDepartment of Mechanical Science and Engineering, University of Illinois at Urbana-Champaign, Urbana, Illinois 61801, USA

† Electronic supplementary information (ESI) available. See DOI: 10.1039/c9sc06582b

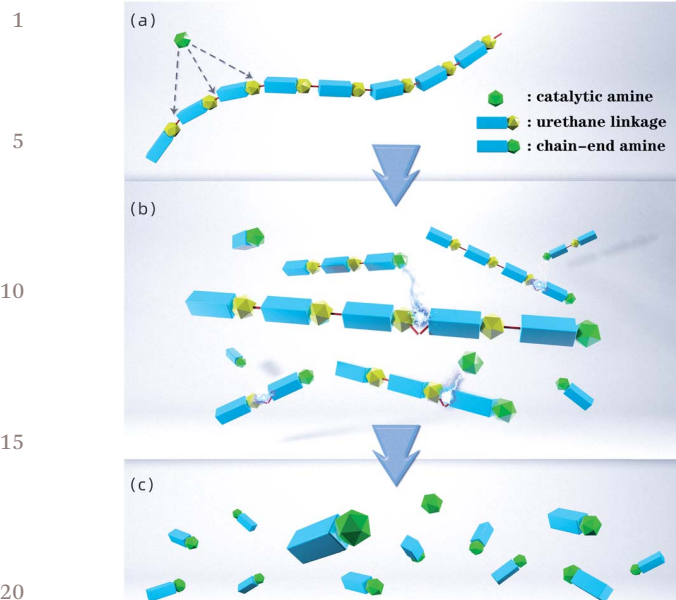
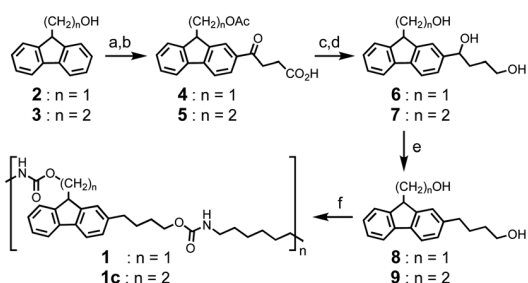


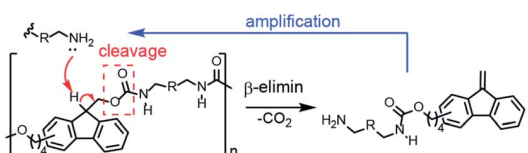
Fig. 1 (a) Design of base-triggered self-amplifying degradable polyurethane that have higher sensitivity to catalytic amount of base and have autocatalytic degradation mechanism.



Scheme 1 Reagents and conditions: (a) acetic anhydride, pyridine, DCM, 25 °C; (b) succinic anhydride, AlCl_3 , DCM, 0 °C to 25 °C (56% for 4 and 59% for 5); (c) 18% HCl, acetone, reflux; (d) $\text{BH}_3\text{-THF}$, THF, 25 °C (32% for 6 and 34% for 7); (e) Et_3SiH , $\text{BF}_3\text{-OEt}_2$, 0 °C (30% for 8 and 25% for 9); (f) hexamethylene diisocyanate, DBTDL, NMP, 25 °C (75% for 1 and 70% for 1c).

Et_3SiH . Traditional polycondensation was performed with a 1 : 1 ratio of diol monomer and hexylmethylene diisocyanate to afford polymer 1 and 1c.

As illustrated in Scheme 2, the addition of base can abstract the weakly acidic fluorenyl methine proton on the polymer 1 backbone, followed by E1cB elimination and decarboxylation to



Scheme 2 Degradation mechanism of base-triggered self-amplifying degradable polyurethane.

generate a dibenzofulvene and stoichiometric amine that can catalyse additional cleavage reactions before or after addition to the dibenzofulvene unit. The two polyurethanes 1 and 1c are identical structurally except that control polymer 1c is unable to undergo base-triggered degradation because the additional methylene group prevents the E1cB elimination from occurring. Both 1 and 1c were characterized by gel permeation chromatography (GPC) with DMF as the eluent (Fig. S6 and S7†). Polymer 1 has a $M_n = 22$ kDa ($D = 2.1$) and control polymer 1c has $M_n = 11$ kDa ($D = 2.6$). The ^1H NMR was consistent with the expected structure of 1 (Fig. S3†) and 1c (Fig. S4†).

Thermal gravimetric analysis (TGA) of polymer 1 and polymer 1c revealed the onset of thermal degradation to occur around 120 °C and 280 °C respectively (Fig. S25 and S26†) and the onset thermal temperature at 120 °C of polymer 1 correlates well to what Simeunovic and his coworkers reported.³³ The T_g of polymer 1 and 1c were determined to be 61 °C and 45 °C, respectively, the later value measured by differential scanning calorimetry (DSC) (Fig. S27†).

Several bases were found to trigger the autocatalytic degradation of 1 (Fig. S11†), with hexylamine chosen for further study because its basicity and steric hindrance is most similar to the amplified amine species. Thus, the base-triggered degradation of polymers 1 and 1c in DMF solution was initiated by the addition of hexylamine and monitored by gel permeation chromatography (GPC). When 1 was exposed to 5 mol% hexylamine (per repeat unit), it showed a progressive and significant decrease in molecular weight over a 12 h period. As seen in Fig. 2a, the reduction in polymer size over time is nonlinear. Thus, the retention time of the 1 shifts only 1 min during the first 2 h but between 6 h and 9 h significantly broadens and shifts to longer times. In contrast, under the same conditions, the GPC of polymer 1c remained unchanged over 24 h (Fig. S8†).

^1H NMR was used to monitor the molecular details of the degradation of polymers 1 and 1c in the presence of hexylamine in $\text{DMSO}-d_6$ solution. Consistent with the GPC study, no change in the NMR of 1c was observed over 24 h with 5 mol% hexylamine (Fig. S10†). In the case of 1, addition of 5 mol% of hexylamine led to the simultaneous disappearance of the methine and methylene protons labelled a and b at δ 4.33 and 4.16 ppm, respectively and the appearance of alkene protons at δ 6.25 ppm from the dibenzofulvene elimination product (Fig. 2b and S9†).

To determine how the concentration of the base trigger affects the rate of the degradation, quantitative ^1H NMR-monitored kinetics were carried out in the presence of 0.5 mol%, 1 mol%, 5 mol%, 20 mol% and 100 mol% hexylamine. As seen in Fig. 2c, a stoichiometric amount of hexylamine induced complete polymer degradation at room temperature within 1 h. The rate profile and time for complete degradation correlated with the amount of base trigger. Thus, with no added base the polymer was stable, whereas for 0.5 mol%, 1 mol%, 5 mol%, 20 mol% and 100 mol% hexylamine the degradation reached 90% at *ca.* 47 min, 2 h, 10 h, 12 h, and 15 h, respectively. Most excitingly was the observation that the three low hexylamine experiments (0.5 to 5 mol%) exhibited obvious induction periods and sigmoidal conversion curves indicative of autocatalytic degradation.

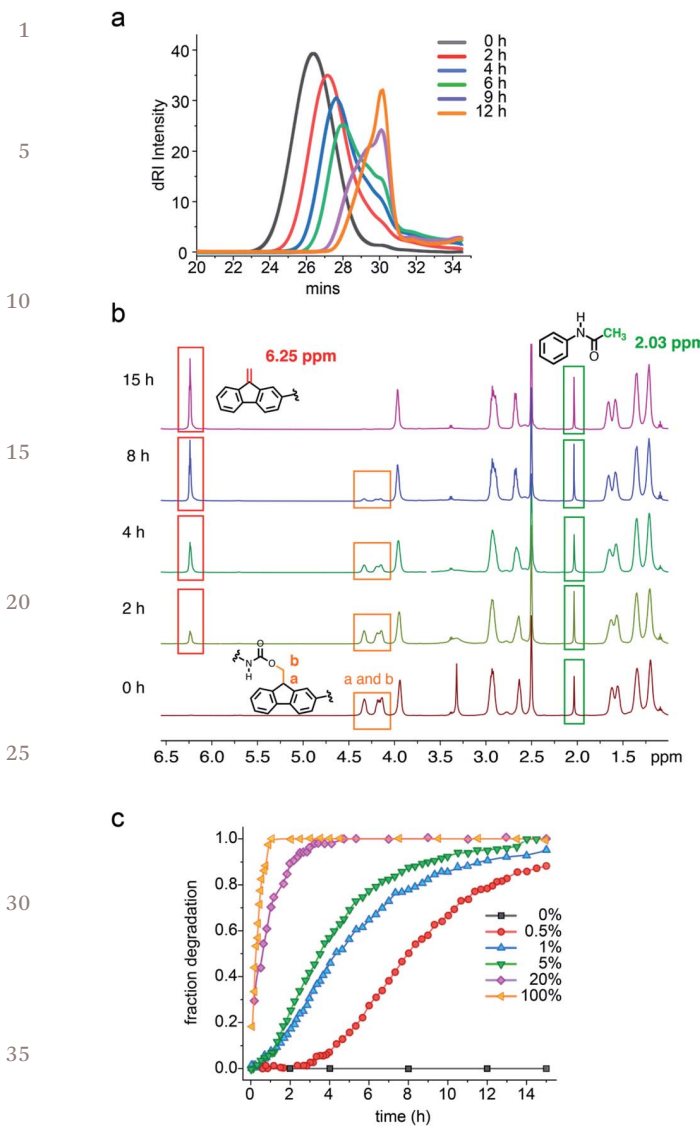


Fig. 2 (a) GPC of **1** over time after addition of 5 mol% hexylamine (per repeat unit). (b) Time-dependent ¹H NMR spectra of **1** in DMSO-*d*₆ with 5 mol% hexylamine as trigger and acetamide as internal standard. (c) ¹H NMR degradation of **1** over time with different hexylamine concentrations. Orange: 100 mol%, purple: 20 mol%, green: 5 mol%, blue: 1 mol%, red: 0.5 mol%, gray: 0 mol%. Fraction degradation calculated from ratio of signals at δ 6.25 or 4.25 ppm (alkene product or a/b protons of starting polymer) and internal standard at 2.03 ppm. Lines connecting the points are to guide the eyes.

Additional support for the autocatalytic, base amplification mechanism came from fitting the degradation data of polymer **1** to an autocatalytic kinetic model (eqn (S3)†).^{23,24,34–36} In this model, rate constants k_1 and k_2 separately represent the non-autocatalytic and autocatalytic, amine-accelerated rate constants (see ESI† for details). Consistent with the mechanism shown in Scheme 2, fitting the sigmoidal curves seen in Fig. 2c, led to k_2 values that were quite close and $k_2 c_0$ values that are larger than the k_1 values (Table 1). The latter is especially true for the 0.5 mol% hexylamine run, in which the $k_2 c_0$ ($6.7 \times 10^{-3} \text{ min}^{-1}$) is 30 times larger than k_1 ($2.1 \times 10^{-4} \text{ min}^{-1}$). This

Table 1 Calculated rate constants for the nonautocatalytic and autocatalytic pathways of the degradation of linear polymer at room temperature (see Fig. S14–S16)†

Trigger	$k_1 (\text{min}^{-1})$	$k_2 (\text{M}^{-1} \text{ min}^{-1})$	$k_2 c_0 (\text{min}^{-1})$
0.5%	2.1×10^{-4}	0.28	6.7×10^{-3}
1%	1.4×10^{-3}	0.19	4.3×10^{-3}
5%	1.8×10^{-3}	0.23	5.6×10^{-3}

† Rate constants k_1 and k_2 are defined in text, c_0 is initial concentration of degradable group. Concentration (M) is [Fmoc]. See ESI for additional details of the kinetic fit. The 1 mol% run was repeated and values found within 20%, establishing reproducibility.

larger $k_2 c_0$ value is characteristic of an autocatalytic reaction (Table 1 and Fig. S14–S16)†.

To further characterize the degradation of **1**, liquid chromatography coupled mass spectrometry (LC-MS) was utilized to identify the major degradation products, and further indicate the chemical structure of the polymer repeating units. Analysis of the degradation products from polymer **1** through LC-MS revealed two major peaks, degradation product 1 with higher intensity appearing at 6.4 min ($m/z = 393.4$) and degradation product 2 with a lower intensity appearing at 9.3 min ($m/z = 669.4$) (Fig. S12)†. These products are consistent with two types of repeating units in **1** (Fig. 3) and degradation product 1

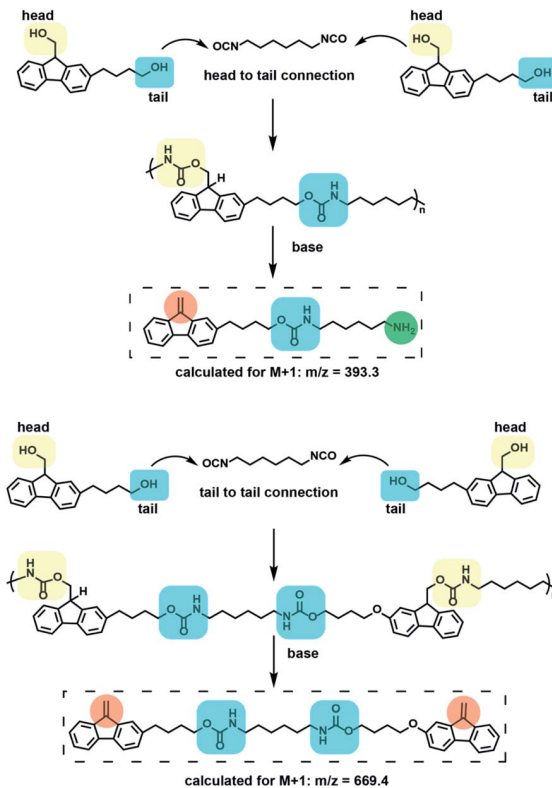


Fig. 3 (a) Major repeating unit formed by head to tail connection and its corresponding degradation product observed by LC-MS. (b) Minor repeating units formed by tail to tail connection and its corresponding degradation product observed by LC-MS.

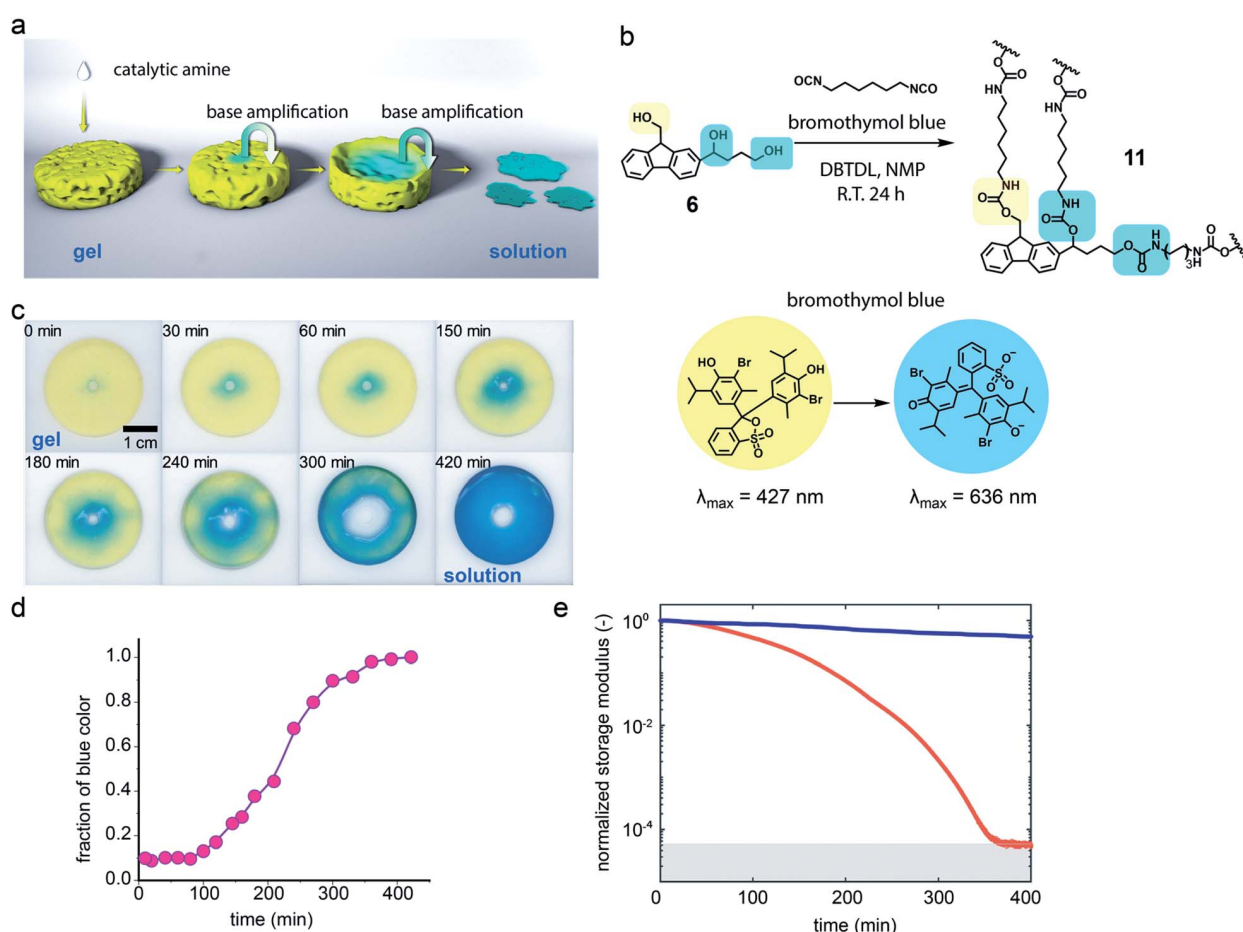
1 demonstrates the ability of polymer **1** to form amine products *via* Fmoc deprotection.

5 Polyurethanes are important and widely used polymeric materials commonly found in plastics, adhesives and coatings.^{37,38} Unlike polymer **1**, these materials are usually prepared from a polyol that produces cross-linking. The combination of cross-linking and the stability of the urethane linkage makes poly-urethanes highly durable but also limits their end-of-life break-down. To examine whether the base-amplified degradation 10 might be applicable to bulk materials, triol **6** was prepared (see ESI†) and polymerized with hexamethylene diisocyanate and dibutyltindilaurate (DBTDL) as catalyst in *N*-methylpyrrolidone (NMP) with bromothymol blue present to visualize the gel and provide a pH indicator (Fig. 4b and S17†). The polymerization was performed at room temperature in a circular Teflon mold for 24 h to give a polyurethane film of **11** with a 500 μm thickness.

15 To characterize the polymer film, it was immersed in additional NMP which induced significant swelling, but did not dissolve the gel. This observation is consistent with a cross-linked gel. To demonstrate the urethane network, the polymer

1 film was dried under high vacuum and characterized by attenuated total reflection infrared spectroscopy (ATR-FTIR). The absorption peak at 1694 cm^{-1} and 1252 cm^{-1} were assigned to the urethane structure and the absorption peak at 3326 cm^{-1} was assigned to unreacted hydroxyl groups in the polymer network (Fig. S18†).³⁹

5 Degradation study of the polymer film was performed with film being swelled by NMP solution. In the degradation study, the centre of the polymer film changed from yellow to blue after 2 μL 180 mM hexylamine NMP solution was added in the centre and photographs were acquired over time (Fig. 4c). It was observed that the degradation area kept increasing, producing a deep blue colour, suggesting the formation of increasing numbers of terminal amino groups with conversion of the bromothymol blue pH indicator to its blue colour ring open form. Quantification of the degradation area with blue colour change for the polymer film was assisted by the Image-Pro Plus 10 (Fig. 4d). An increase in degradation area also simulates a sigmoidal curve, with a nonlinear increase from 10% at 100 min to 90% at 300 min, which is consistent with an auto-catalytic degradation process for the crosslinked gel. The



1
5
10
15
20
25
30
35
40
45
50
55
100
150
200
250
300
350
400
450
500
550
600
650
700
750
800
850
900
950
1000
1050
1100
1150
1200
1250
1300
1350
1400
1450
1500
1550
1600
1650
1700
1750
1800
1850
1900
1950
2000
2050
2100
2150
2200
2250
2300
2350
2400
2450
2500
2550
2600
2650
2700
2750
2800
2850
2900
2950
3000
3050
3100
3150
3200
3250
3300
3350
3400
3450
3500
3550
3600
3650
3700
3750
3800
3850
3900
3950
4000
4050
4100
4150
4200
4250
4300
4350
4400
4450
4500
4550
4600
4650
4700
4750
4800
4850
4900
4950
5000
5050
5100
5150
5200
5250
5300
5350
5400
5450
5500
5550
5600
5650
5700
5750
5800
5850
5900
5950
6000
6050
6100
6150
6200
6250
6300
6350
6400
6450
6500
6550
6600
6650
6700
6750
6800
6850
6900
6950
7000
7050
7100
7150
7200
7250
7300
7350
7400
7450
7500
7550
7600
7650
7700
7750
7800
7850
7900
7950
8000
8050
8100
8150
8200
8250
8300
8350
8400
8450
8500
8550
8600
8650
8700
8750
8800
8850
8900
8950
9000
9050
9100
9150
9200
9250
9300
9350
9400
9450
9500
9550
9600
9650
9700
9750
9800
9850
9900
9950
10000
10050
10100
10150
10200
10250
10300
10350
10400
10450
10500
10550
10600
10650
10700
10750
10800
10850
10900
10950
11000
11050
11100
11150
11200
11250
11300
11350
11400
11450
11500
11550
11600
11650
11700
11750
11800
11850
11900
11950
12000
12050
12100
12150
12200
12250
12300
12350
12400
12450
12500
12550
12600
12650
12700
12750
12800
12850
12900
12950
13000
13050
13100
13150
13200
13250
13300
13350
13400
13450
13500
13550
13600
13650
13700
13750
13800
13850
13900
13950
14000
14050
14100
14150
14200
14250
14300
14350
14400
14450
14500
14550
14600
14650
14700
14750
14800
14850
14900
14950
15000
15050
15100
15150
15200
15250
15300
15350
15400
15450
15500
15550
15600
15650
15700
15750
15800
15850
15900
15950
16000
16050
16100
16150
16200
16250
16300
16350
16400
16450
16500
16550
16600
16650
16700
16750
16800
16850
16900
16950
17000
17050
17100
17150
17200
17250
17300
17350
17400
17450
17500
17550
17600
17650
17700
17750
17800
17850
17900
17950
18000
18050
18100
18150
18200
18250
18300
18350
18400
18450
18500
18550
18600
18650
18700
18750
18800
18850
18900
18950
19000
19050
19100
19150
19200
19250
19300
19350
19400
19450
19500
19550
19600
19650
19700
19750
19800
19850
19900
19950
20000
20050
20100
20150
20200
20250
20300
20350
20400
20450
20500
20550
20600
20650
20700
20750
20800
20850
20900
20950
21000
21050
21100
21150
21200
21250
21300
21350
21400
21450
21500
21550
21600
21650
21700
21750
21800
21850
21900
21950
22000
22050
22100
22150
22200
22250
22300
22350
22400
22450
22500
22550
22600
22650
22700
22750
22800
22850
22900
22950
23000
23050
23100
23150
23200
23250
23300
23350
23400
23450
23500
23550
23600
23650
23700
23750
23800
23850
23900
23950
24000
24050
24100
24150
24200
24250
24300
24350
24400
24450
24500
24550
24600
24650
24700
24750
24800
24850
24900
24950
25000
25050
25100
25150
25200
25250
25300
25350
25400
25450
25500
25550
25600
25650
25700
25750
25800
25850
25900
25950
26000
26050
26100
26150
26200
26250
26300
26350
26400
26450
26500
26550
26600
26650
26700
26750
26800
26850
26900
26950
27000
27050
27100
27150
27200
27250
27300
27350
27400
27450
27500
27550
27600
27650
27700
27750
27800
27850
27900
27950
28000
28050
28100
28150
28200
28250
28300
28350
28400
28450
28500
28550
28600
28650
28700
28750
28800
28850
28900
28950
29000
29050
29100
29150
29200
29250
29300
29350
29400
29450
29500
29550
29600
29650
29700
29750
29800
29850
29900
29950
30000
30050
30100
30150
30200
30250
30300
30350
30400
30450
30500
30550
30600
30650
30700
30750
30800
30850
30900
30950
31000
31050
31100
31150
31200
31250
31300
31350
31400
31450
31500
31550
31600
31650
31700
31750
31800
31850
31900
31950
32000
32050
32100
32150
32200
32250
32300
32350
32400
32450
32500
32550
32600
32650
32700
32750
32800
32850
32900
32950
33000
33050
33100
33150
33200
33250
33300
33350
33400
33450
33500
33550
33600
33650
33700
33750
33800
33850
33900
33950
34000
34050
34100
34150
34200
34250
34300
34350
34400
34450
34500
34550
34600
34650
34700
34750
34800
34850
34900
34950
35000
35050
35100
35150
35200
35250
35300
35350
35400
35450
35500
35550
35600
35650
35700
35750
35800
35850
35900
35950
36000
36050
36100
36150
36200
36250
36300
36350
36400
36450
36500
36550
36600
36650
36700
36750
36800
36850
36900
36950
37000
37050
37100
37150
37200
37250
37300
37350
37400
37450
37500
37550
37600
37650
37700
37750
37800
37850
37900
37950
38000
38050
38100
38150
38200
38250
38300
38350
38400
38450
38500
38550
38600
38650
38700
38750
38800
38850
38900
38950
39000
39050
39100
39150
39200
39250
39300
39350
39400
39450
39500
39550
39600
39650
39700
39750
39800
39850
39900
39950
40000
40050
40100
40150
40200
40250
40300
40350
40400
40450
40500
40550
40600
40650
40700
40750
40800
40850
40900
40950
41000
41050
41100
41150
41200
41250
41300
41350
41400
41450
41500
41550
41600
41650
41700
41750
41800
41850
41900
41950
42000
42050
42100
42150
42200
42250
42300
42350
42400
42450
42500
42550
42600
42650
42700
42750
42800
42850
42900
42950
43000
43050
43100
43150
43200
43250
43300
43350
43400
43450
43500
43550
43600
43650
43700
43750
43800
43850
43900
43950
44000
44050
44100
44150
44200
44250
44300
44350
44400
44450
44500
44550
44600
44650
44700
44750
44800
44850
44900
44950
45000
45050
45100
45150
45200
45250
45300
45350
45400
45450
45500
45550
45600
45650
45700
45750
45800
45850
45900
45950
46000
46050
46100
46150
46200
46250
46300
46350
46400
46450
46500
46550
46600
46650
46700
46750
46800
46850
46900
46950
47000
47050
47100
47150
47200
47250
47300
47350
47400
47450
47500
47550
47600
47650
47700
47750
47800
47850
47900
47950
48000
48050
48100
48150
48200
48250
48300
48350
48400
48450
48500
48550
48600
48650
48700
48750
48800
48850
48900
48950
49000
49050
49100
49150
49200
49250
49300
49350
49400
49450
49500
49550
49600
49650
49700
49750
49800
49850
49900
49950
50000
50050
50100
50150
50200
50250
50300
50350
50400
50450
50500
50550
50600
50650
50700
50750
50800
50850
50900
50950
51000
51050
51100
51150
51200
51250
51300
51350
51400
51450
51500
51550
51600
51650
51700
51750
51800
51850
51900
51950
52000
52050
52100
52150
52200
52250
52300
52350
52400
52450
52500
52550
52600
52650
52700
52750
52800
52850
52900
52950
53000
53050
53100
53150
53200
53250
53300
53350
53400
53450
53500
53550
53600
53650
53700
53750
53800
53850
53900
53950
54000
54050
54100
54150
54200
54250
54300
54350
54400
54450
54500
54550
54600
54650
54700
54750
54800
54850
54900
54950
55000
55050
55100
55150
55200
55250
55300
55350
55400
55450
55500
55550
55600
55650
55700
55750
55800
55850
55900
55950
56000
56050
56100
56150
56200
56250
56300
56350
56400
56450
56500
56550
56600
56650
56700
56750
56800
56850
56900
56950
57000
57050
57100
57150
57200
57250
57300
57350
57400
57450
57500
57550
57600
57650
57700
57750
57800
57850
57900
57950
58000
58050
58100
58150
58200
58250
58300
58350
58400
58450
58500
58550
58600
58650
58700
58750
58800
58850
58900
58950
59000
59050
59100
59150
59200
59250
59300
59350
59400
59450
59500
59550
59600
59650
59700
59750
59800
59850
59900
59950
60000
60050
60100
60150
60200
60250
60300
60350
60400
60450
60500
60550
60600
60650
60700
60750
60800
60850
60900
60950
61000
61050
61100
61150
61200
61250
61300
61350
61400
61450
61500
61550
61600
61650
61700
61750
61800
61850
61900
61950
62000
62050
62100
62150
62200
62250
62300
62350
62400
62450
62500
62550
62600
62650
62700
62750
62800
62850
62900
62950
63000
63050
63100
63150
63200
63250
63300
63350
63400
63450
63500
63550
63600
63650
63700
63750
63800
63850
63900
63950
64000
64050
64100
64150
64200
64250
64300
64350
64400
64450
64500
64550
64600
64650
64700
64750
64800
64850
64900
64950
65000
65050
65100
65150
65200
65250
65300
65350
65400
65450
65500
65550
65600
65650
65700
65750
65800
65850
65900
65950
66000
66050
66100
66150
66200
66250
66300
66350
66400
66450
66500
66550
66600
66650
66700
66750
66800
66850
66900
66950
67000
67050
67100
67150
67200
67250
67300
67350
67400
67450
67500
67550
67600
67650
67700
67750
67800
67850
67900
67950
68000
68050
68100
68150
68200
68250
68300
68350
68400
68450
68500
68550
68600
68650
68700
68750
68800
68850
68900
68950
69000
69050
69100
69150
69200
69250
69300
69350
69400
69450
69500
69550
69600
69650
69700
69750
69800
69850
69900
69950
70000
70050
70100
70150
70200
70250
70300
70350
70400
70450
70500
70550
70600
70650
70700
70750
70800
70850
70900
70950
71000
71050
71100
71150
71200
71250
71300
71350
71400
71450
71500
71550
71600
71650
71700
71750
71800
71850
71900
71950
72000
72050
72100
72150
72200
72250
72300
72350
72400
72450
72500
72550
72600
72650
72700
72750
72800
72850
72900
72950
73000
73050
73100
73150
73200
73250
73300<br

complete degradation of the polymer film required 420 min and over this period the yellow solid film became a blue solution (see ESI Video†). Six prominent degradation products were observed and characterised by high resolution electrospray ionization mass spectrometry (HR-ESI-MS, see Fig. S19†). Three of the six degradation products must contain a urethane structure at the benzylic position, consistent with the proposed cross-linked structure. Several of the degradation products have *m/z* values indicative of dibenzofulvene units or amino groups and this observation is consistent with the proposed Fmoc degradation mechanism.

The degradation process was also monitored by rheology. The storage modulus of the gel was measured and no major rheological change was observed from the polymeric network without addition of the base trigger (blue curve, Fig. 4e and S23†). However, the bulk polymeric network underwent a rapid decrease in storage modulus from about 5300 Pa to nearly 0 Pa upon addition of a very small amount of a dilute hexylamine solution in NMP at room temperature (red curve, Fig. 4e and S23†). In this case autocatalytic equations (eqn (S4) and (S5)†) that relate the storage modulus to degradation time were utilized to quantify the gel breakdown kinetics as described in more detail in the ESI.† In particular, these equations relate the storage modulus decrease to the concentration of crosslinks, thus enabling inference of apparent chemical rate constants. The fitting of triplicate runs (Fig. S24†) gave $k_2 c_0 = 15.9 \pm 5.3 \text{ min}^{-1}$, which is much larger than the $k_1 = 2.1 \times 10^{-3} \pm 1.1 \times 10^{-3} \text{ min}^{-1}$. These observations are consistent with an autocatalytic degradation process.

Conclusion

In conclusion, we developed a new type of self-amplifying degradable polymer with self-accelerating degradation properties using the well-developed base-sensitive Fmoc protecting group used in peptide synthesis. The incorporation of Fmoc in every repeating unit provides extremely sensitive polymeric materials with a small amount of base leading to rapid and amplified degradation. The base amplification process may be useful in applications where rapid production of an amine base is desirable. The crosslinked gel provides a rare example where a tiny local stimulation generates long range, rapid macroscopic degradation. In principle such a degradation might propagate over very large distances. Our current efforts are focused on generalizing this self-amplified degradation process to other kinds of triggers such as light, ions, and ROX agents.

Conflicts of interest

There are no conflicts to declare.

Acknowledgements

This work is partially supported by the National Science Foundation (NSF CHE-1709718) and the National Institutes of Health (R01 AR069645).

Notes and references

- N. Kamaly, B. Yameen, J. Wu and O. C. Farokhzad, *Chem. Rev.*, 2016, **116**, 2602–2663.
- A. P. Esser-Kahn, S. A. Odom, N. R. Sottos, S. R. White and J. S. Moore, *Macromolecules*, 2011, **44**, 5539–5553.
- J. Li and D. J. Mooney, *Nat. Rev. Mater.*, 2016, **1**, 16071–16087.
- K. K. Fu, Z. Wang, J. Dai, M. Carter and L. Hu, *Chem. Mater.*, 2016, **28**, 3527–3539.
- E. R. Gillies and J. M. Fréchet, *Drug Discovery Today*, 2005, **10**, 35–43.
- J. Hu and S. Liu, *Macromolecules*, 2010, **43**, 8315–8330.
- Y. Zhang, Q. Yin, L. Yin, L. Ma, L. Tang and J. Cheng, *Angew. Chem., Int. Ed.*, 2013, **52**, 6435–6439.
- Y. Zhang, L. Ma, X. Deng and J. Cheng, *Polym. Chem.*, 2013, **4**, 224–228.
- K. Cai, J. Yen, Q. Yin, Y. Liu, Z. Song, S. Lezmi, Y. Zhang, X. Yang, W. G. Helferich and J. Cheng, *Biomater. Sci.*, 2015, **3**, 1061–1065.
- S. Gnaim and D. Shabat, *J. Am. Chem. Soc.*, 2017, **139**, 10002–10008.
- A. P. Esser-Kahn, N. R. Sottos, S. R. White and J. S. Moore, *J. Am. Chem. Soc.*, 2010, **132**, 10266–10268.
- M. G. Olah, J. S. Robbins, M. S. Baker and S. T. Phillips, *Macromolecules*, 2013, **46**, 5924–5928.
- K. Yeung, H. Kim, H. Mohapatra and S. T. Phillips, *J. Am. Chem. Soc.*, 2015, **137**, 5324–5327.
- B. Fan, J. F. Trant, A. D. Wong and E. R. Gillies, *J. Am. Chem. Soc.*, 2014, **136**, 10116–10123.
- N. Fomina, C. McFearin, M. Sermsakdi, O. Edigin and A. Almutairi, *J. Am. Chem. Soc.*, 2010, **132**, 9540–9542.
- C. de Gracia Lux, S. Joshi-Barr, T. Nguyen, E. Mahmoud, E. Schopf, N. Fomina and A. Almutairi, *J. Am. Chem. Soc.*, 2012, **134**, 15758–15764.
- X. Sun, S. D. Dahlhauser and E. V. Anslyn, *J. Am. Chem. Soc.*, 2017, **139**, 4635–4638.
- J.-A. Gu, V. Mani and S.-T. Huang, *Analyst*, 2015, **140**, 346–352.
- M. S. Baker and S. T. Phillips, *J. Am. Chem. Soc.*, 2011, **133**, 5170–5173.
- X. Sun, D. Shabat, S. T. Phillips and E. V. Anslyn, *J. Phys. Org. Chem.*, 2018, **31**, e3827.
- X. Sun and E. V. Anslyn, *Angew. Chem., Int. Ed.*, 2017, **56**, 9522–9526.
- H. Kim, M. S. Baker and S. T. Phillips, *Chem. Sci.*, 2015, **6**, 3388–3392.
- H. Mohapatra, H. Kim and S. T. Phillips, *J. Am. Chem. Soc.*, 2015, **137**, 12498–12501.
- K. A. Miller, E. G. Morado, S. R. Samanta, B. A. Walker, A. Z. Nelson, S. Sen, D. T. Tran, D. J. Whitaker, R. H. Ewoldt, P. V. Braun and S. C. Zimmerman, *J. Am. Chem. Soc.*, 2019, **141**, 2838–2842.
- Anon, *Nature*, 2019, **566**, 157.
- C. M. Possanza Casey and J. S. Moore, *ACS Macro Lett.*, 2016, **5**, 1257–1260.

1 27 H.-C. Wang, Y. Zhang, C. M. Possanza, S. C. Zimmerman, J. Cheng, J. S. Moore, K. Harris and J. S. Katz, *ACS Appl. Mater. Interfaces*, 2015, **7**, 6369–6382.

5 28 K. Arimitsu, M. Miyamoto and K. Ichimura, *Angew. Chem., Int. Ed.*, 2000, **39**, 3425–3428.

10 29 H. Mohapatra, K. M. Schmid and S. T. Phillips, *Chem. Commun.*, 2012, **48**, 3018–3020.

15 30 K. Arimitsu and K. Ichimura, *J. Mater. Chem.*, 2004, **14**, 336–343.

20 31 K. Arimitsu, K. Tomota, S. Fuse, K. Kudo and M. Furutani, *RSC Adv.*, 2016, **6**, 38388–38390.

25 32 K. Arimitsu, H. Kitamura, R. Mizuochi and M. Furutani, *Chem. Lett.*, 2015, **44**, 309–311.

30 33 S. Höck, R. Marti, R. Riedl and M. Simeunovic, *Chimia*, 2010, **64**, 200–202.

35 34 F. Mata-Perez and J. F. Perez-Benito, *J. Chem. Educ.*, 1987, **64**, 925–927.

40 35 O. P. Lee, H. Lopez Hernandez and J. S. Moore, *ACS Macro Lett.*, 2015, **4**, 665–668.

45 36 J. F. Perez-Benito, *J. Phys. Chem. A*, 2011, **115**, 9876–9885.

50 37 H.-W. Engels, H.-G. Pirkl, R. Albers, R. W. Albach, J. Krause, A. Hoffmann, H. Casselmann and J. Dormish, *Angew. Chem., Int. Ed.*, 2013, **52**, 9422–9441.

55 38 F. E. Golling, R. Pires, A. Hecking, J. Weikard, F. Richter, K. Danielmeier and D. Dijkstra, *Polym. Int.*, 2019, **68**, 848–855.

60 39 H. Hao, J. Shao, Y. Deng, S. He, F. Luo, Y. Wu, J. Li, H. Tan, J. Li and Q. Fu, *Biomater. Sci.*, 2016, **4**, 1682–1690.